

PATRONUS: SAFEGUARDING TEXT-TO-IMAGE MODELS AGAINST WHITE-BOX ADVERSARIES

Anonymous authors

Paper under double-blind review

ABSTRACT

Text-to-image (T2I) models, though exhibiting remarkable creativity in image generation, may be exploited to produce unsafe images. Existing safety measures, e.g., content moderation or model alignment, fail in the presence of white-box adversaries who know and can adjust model parameters, e.g., by fine-tuning. This paper presents a novel defensive framework, named PATRONUS, which equips T2I models with holistic protection to defend against white-box adversaries. Specifically, we design an internal moderator that decodes unsafe input features into zero vectors while ensuring the decoding performance of benign input features. Furthermore, we strengthen the model alignment with a carefully designed non-fine-tunable learning (NFTL) mechanism, ensuring the T2I model will not be compromised by malicious fine-tuning. We have conducted extensive experiments to validate the intactness of the performance on safe content generation and the effectiveness to reject unsafe content generation. Experiment results have confirmed the resistance of PATRONUS against various fine-tuning attacks by white-box adversaries.

1 INTRODUCTION

Text-to-image (T2I) models (Rombach et al., 2022; LMU, b; mid; Inc.) dazzle us with their stunning performance and amazing creativity. However, ethical issues with T2I models regarding unsafe content generation, like sexual-explicit, violent, and political images (Williams, 2023; Milmo, 2023; McQueen, 2023; Hunter, 2023a;b), are also alarming. An unprotected T2I model can easily be prompted to generate a large number of unsafe images. The Internet Watch Foundation discovered that countless images of child sexual abuse produced by T2I models had been distributed on the dark web (Milmo, 2023), causing potential sexual exploitation and sexual abuse (McQueen, 2023; Hunter, 2023a;b). Therefore, shielding T2I models from being exploited for unsafe image generation has significant research implications.

Existing defenses can be classified into two categories, *i.e.*, content moderation (Li; LMU, a) and model alignment (Schramowski et al., 2023; Gandikota et al., 2023). Content moderation aims to detect and block unsafe input prompts (Li) or output images (LMU, a). This is achieved mainly by input filters, output filters, or both. However, the filters are usually external to the T2I model and can be easily removed by white-box adversaries at the code level (Reddit, 2022). Model alignment aims to fine-tune the T2I model to eliminate its learned unsafe concept (Schramowski et al., 2023; Gandikota et al., 2023). Though being internally resistant to unsafe content generation, safely-aligned models are easily corrupted by fine-tuning with a small number of unsafe images.

In this paper, we propose PATRONUS, a defensive framework that strengthens the diffusion and decoder modules of a pre-trained T2I model. The design goal of PATRONUS is three-fold. (1) *Rejection of unsafe content generation*. The protected model should refuse to output unsafe content. (2) *Resistance to malicious fine-tuning*. The protected model should refuse to output unsafe content even if the model is fine-tuned with unsafe samples. (3) *Intact performance of benign content*. The protected model should preserve the performance regarding benign content. The workflow of PATRONUS is illustrated in Figure 1.

Rejection of unsafe content generation. Compared with input moderation, output moderation does not depend on input prompts and is more generalizable to unseen malicious prompts. Therefore, we devise a conditional decoder, which decodes only benign generations from the diffusion module (*i.e.*,

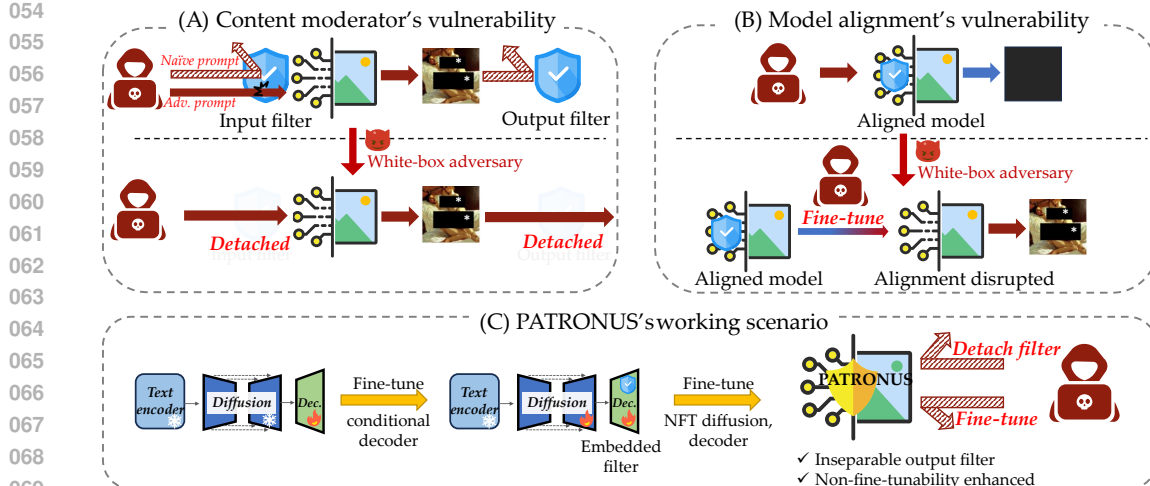


Figure 1: The objective of PATRONUS. 1) Inseparable moderation that defeats the adversary’s detaching process. 2) Non-fine-tunable safety mechanism that defeats the adversary’s malicious fine-tuning.

processing of the input) but refuses unsafe ones. This conditional decoder is inseparable from the T2I model. We achieve this through a prompt-independent fine-tuning on the decoder. Specifically, we input unsafe images into the encoder to collect unsafe features and then direct the decoder’s decoding of these features to zero vectors. In this way, we assure the generalizability of the decoder’s defensive capabilities against unsafe features.

Resistance to malicious fine-tuning. White-box adversaries may use a diversity of fine-tuning techniques to corrupt the moderated T2I model. Inspired by the idea of adversarial training, we align the moderated model through a min-max game, simulating a worst-case adversary who attempts to regain unsafe content generation with malicious fine-tuning. The min optimization mimics the adversarial goal of decreasing the performance loss on unsafe samples, and the max optimization aims to suppress the fine-tuned performance obtained in the min optimization. To achieve generalization, we construct a bag of fine-tuning strategies, including different optimizers, learning rates, iterations, batch sizes, and training sizes. Through a mixed sampling of fine-tuning strategies, the model’s robustness and generalization to different fine-tuning processes are improved.

Intact performance of benign content. The performance of benign prompts may be degraded during the model alignment process. To tackle this difficulty, we utilize multi-task learning to achieve a balance between the performance of safe content generation and the resistance to unsafe content generation by adaptively computing appropriate weighting coefficients for these two objectives.

Extensive experiments have been conducted to evaluate the performance of PATRONUS. For I2P and SneakyPrompt datasets, PATRONUS can maintain the CLIP score of unsafe prompts to as low as 16.5 (visually black images) even after 500 malicious fine-tuning iterations. We demonstrate that it is hard to allure our protected model to produce unsafe content using any trick, and the cost of instigating an attack on our model is relatively high. We will open-source our code in the hope of incentivizing more research in the field of AI ethics.

We summarize our theoretical and technical contributions as follows:

- We make the pioneer attempt to investigate and validate the feasibility of a defense against white-box adversaries for T2I models. We innovatively apply the concept of non-fine-tunable learning to the T2I scenario.
- We design an inseparable content moderation mechanism that is prompt-independent. Additionally, our approach can resist malicious fine-tuning within a given budget, imposing significant costs on the adversary.
- We conduct extensive experiments to verify the effectiveness and robustness of PATRONUS against a diversity of adversarial prompts and malicious fine-tuning strategies.

108 **2 BACKGROUND**

110 In this section, we briefly discuss the preliminary knowledge of T2I generation and related work
 111 necessary for illustrating our method. Two lines of defenses are relevant to our study: 1) content
 112 moderation and 2) model alignment.

113 **T2I pipeline:** Consider a T2I pipeline, parameterized by θ (noted as \mathcal{M}_θ), it involves three cascading
 114 modules, text encoder \mathcal{M}_{enc} , diffusion module \mathcal{M}_{diff} , and decoder \mathcal{M}_{dec} , *i.e.*,

$$\mathcal{M}_\theta = \mathcal{M}_{dec} \circ \mathcal{M}_{diff} \circ \mathcal{M}_{enc}. \quad (1)$$

115 Let x^t represent the textual prompt. The text encoder takes x^t as input and results in a conditioning
 116 vector. Then, the diffusion module generates a low-resolution feature with the guidance of the
 117 conditioning vector and participation of noise sampled from the Gaussian distribution. Finally,
 118 the decoder reconstructs the diffusion feature back to the original pixel space, *i.e.*, high-resolution
 119 images.

120 **Content Moderation:** There are two types of content moderators: input filters and output filters.
 121 Input filters are applied before the text encoder, detecting whether the textual prompt contains unsafe
 122 words (Jieli). A T2I equipped with the input filter $\mathcal{F}_i : \mathbb{T}^d : \text{textual space} \rightarrow \mathbb{Y} = \{0, 1\}$.

$$\mathcal{M}'_\theta = \mathcal{M}_\theta \circ \mathcal{F}_i = \mathcal{M}_{dec} \circ \mathcal{M}_{diff} \circ \mathcal{M}_{enc} \circ \mathcal{F}_i. \quad (2)$$

$$\mathcal{M}'_\theta(x^t) = \begin{cases} \emptyset & \text{if } \mathcal{F}_i(x^t) = 1, \\ \mathcal{M}_\theta(x^t) & \text{if } \mathcal{F}_i(x^t) = 0. \end{cases}$$

123 Where $\mathcal{F}_i(x^t) = 1$ (or 0) signifies that the moderator regards x^t contains (or does not contain)
 124 unsafe content. However, the input filters can be easily bypassed by adversarial prompts (Yang
 125 et al., 2023), which fulfill the goals as follows,

$$\mathcal{F}_i(x^t) = 1, \quad \mathcal{F}_i(\hat{x}^t) = 0, \quad \mathcal{M}_\theta(x^t) \approx \mathcal{M}_\theta(\hat{x}^t). \quad (3)$$

126 where x^t, \hat{x}^t represent the original unsafe prompt and the corresponding adversarial prompt, respec-
 127 tively.

128 Output filters, $\mathcal{F}_o : \mathbb{R}^{H \times W \times C} \rightarrow \mathbb{Y} = \{0, 1\}$, can circumvent this issue, enabling more precise
 129 generation moderation since they directly review the compliance of the generated images as

$$\mathcal{M}'_\theta = \mathcal{F}_o \circ \mathcal{M}_\theta = \mathcal{F}_o \circ \mathcal{M}_{dec} \circ \mathcal{M}_{diff} \circ \mathcal{M}_{enc}. \quad (4)$$

$$\mathcal{M}'_\theta(x^t) = \begin{cases} \emptyset & \text{if } \mathcal{F}_o(\mathcal{M}_\theta(x^t)) = 1, \\ \mathcal{M}_\theta(x^t) & \text{if } \mathcal{F}_o(\mathcal{M}_\theta(x^t)) = 0. \end{cases}$$

130 Where $\mathcal{F}_o(\mathcal{M}_\theta(x^t)) = 1$ (or 0) signifies that the moderator regards the output contains (or does not
 131 contain) unsafe content. However, output filters cannot be applied to defend the white-box adversary
 132 due to its structurally separable nature, *i.e.*, the adversary can directly detach \mathcal{F}_o from \mathcal{M}'_θ at the
 133 code level.

134 **Model alignment:** Model alignment family fine-tunes the diffusion module \mathcal{M}_{diff} , parameterized
 135 by θ_{diff} , to improve compliance. SLD (Schramowski et al., 2023) and ESD (Gandikota et al., 2023)
 136 aim to guide the diffusion module away from unsafe regions or suppress harmful concepts during
 137 the denoising process, like:

$$\theta_{diff}^* = \arg \min_{\theta_{diff}} \sum_{x^t \in \mathbb{U}} -\log(\mathcal{M}_{diff}(\mathcal{M}_{enc}(x^t), z)), \quad (5)$$

138 where \mathbb{U} represents the unsafe prompts. However, they rely on predefined prompts to participate in
 139 training or inference to some extent, which means the generalization cannot be guaranteed. Safe-
 140 Gen (Li et al., 2024) identifies the significance of vision-only layers (parameterized by ϕ) to achieve
 141 text-agnostic mitigation and fine-tunes diffusion parameters against adaptive attackers.

$$\phi^* = \arg \min_{\phi \subset \theta_{diff}} \sum_{x^t \in \mathbb{U}} -\log(\mathcal{M}_{diff}(\mathcal{M}_{enc}(x^t), z)), \quad (6)$$

142 Compared with external filters, these methods encode the defensive property into the existing pa-
 143 rameters. However, we find that their defensive performance can be easily corrupted by fine-tuning
 144 with only a dozen unsafe data and iterations.

162 **3 DESIGN GOAL**
 163

164 In this part, we lay out three major goals of PATRONUS. Let p_u, p_b represent unsafe prompts and
 165 benign prompts.

166 **Goal I: Rejection of Unsafe Content.** The model should refrain from generating images that
 167 contain visible malicious semantic information when confronted with unsafe prompts, *i.e.*, $\mathcal{M}_\theta(p_u) =$
 168 \emptyset . \emptyset represents the absence of unsafe concepts, same hereafter.

169 **Goal II: Resistance to Malicious Fine-tuning.** Even after being fine-tuned with unsafe data by an
 170 adversary, the model should still be unable to generate images that contain visible unsafe content,
 171 *i.e.*, $\phi(\mathcal{M}_\theta)(p_u) = \emptyset$.

172 **Goal III: Preservation of Normal Performance.** The model should maintain similar outputs to the
 173 original model when presented with benign prompts, *i.e.*, $\mathcal{M}_\theta(p_b) \approx \mathcal{M}_0(p_b)$.

174 To integrate these goals in a unified framework, we formally formulate PATRONUS as follows,

$$\begin{aligned} & \min_{\theta} \mathbb{E}_{p \sim \mathcal{D}_m, \phi \sim \Phi} \mathcal{S}(p, \phi(\mathcal{M}_\theta)), \\ & \text{s.t. } \mathbb{E}_{p \sim \mathcal{D}_b} (\max \{0, \mathcal{S}(p, \mathcal{M}_0) - \mathcal{S}(p, \mathcal{M}_\theta)\}) < \epsilon, \end{aligned} \quad (7)$$

179 where $\mathcal{D}_m, \mathcal{D}_b, \Phi$ represents the distribution of unsafe prompts, benign prompts, and fine-tuning
 180 processes, respectively. Note that Φ contains the case where the adversary does not fine-tune and
 181 directly prompts. \mathcal{S} is a measure used to assess the quality of generated images, *e.g.*, the CLIP score
 182 (Radford et al., 2021). ϵ is the tolerance of the performance degradation on benign prompts. Since
 183 the constrained optimization problem in Equation 7 is difficult to solve, we introduce the Lagrange
 184 multiplier and solve the corresponding unconstrained optimization problem as

$$\min_{\theta} \mathbb{E}_{p \sim \mathcal{D}_m, \phi \sim \Phi} \mathcal{S}(p, \phi(\mathcal{M}_\theta)) - \lambda \cdot \mathbb{E}_{p \sim \mathcal{D}_b} (\mathcal{S}(p, \mathcal{M}_\theta)). \quad (8)$$

187 In the rest of the paper, we provide an implementation of PATRONUS that can effectively solve the
 188 formulation objective.

190 **4 METHODOLOGY**
 191

192 **4.1 OVERVIEW**
 193

194 **Key Idea:** To tackle the limitations of existing defenses, which can be structurally removed or
 195 disrupted by malicious fine-tuning, we develop PATRONUS. The intuition of PATRONUS contains
 196 three aspects: 1) To achieve structurally inseparable output moderation, we embed the output filter
 197 within the decoder. Specifically, we govern the decoder module, *i.e.*, making it perform conditional
 198 decoding based on the safety of the generated features. 2) To ensure the defensive performance
 199 survives the adversary’s fine-tuning, we enhance the defended components, including the conditional
 200 decoder and the aligned diffusion, with non-fine-tunability. 3) We carefully control the defense
 201 process to exclude the involvement of attack prompts, achieving prompt-independent defense, which
 202 guarantees robustness against various unsafe prompts.

203 **Overall Pipeline:** Starting from a pre-trained T2I pipeline, we implement PATRONUS by fine-tuning
 204 the decoder and the diffusion modules. First, we fine-tune a conditional decoder, which refuses to
 205 decode unsafe features, to achieve an inseparable moderator. Then, we create a non-fine-tunable
 206 safety mechanism to enable the conditional decoder and the aligned U-Net to resist malicious fine-
 207 tuning. Additionally, we pay attention to benign performance preservation that encourages the model
 208 to review the knowledge of benign inputs. Figure 2 describes the pipeline of PATRONUS. We
 209 summarize the overall process of PATRONUS in Algorithm 1.

210 **4.2 INSEPARABLE MODERATOR**
 211

212 In this section, we design and realize an inseparable moderator by fine-tuning a decoder that per-
 213 forms the conditional output based on the feature’s safety. Equivalent to having an output moderator
 214 \mathcal{F}_{emb} embedded internally, the conditional decoder can be formalized as

$$\mathcal{M}'_{dec} = \mathcal{M}_{dec} \odot \mathcal{F}_{emb}. \quad (9)$$

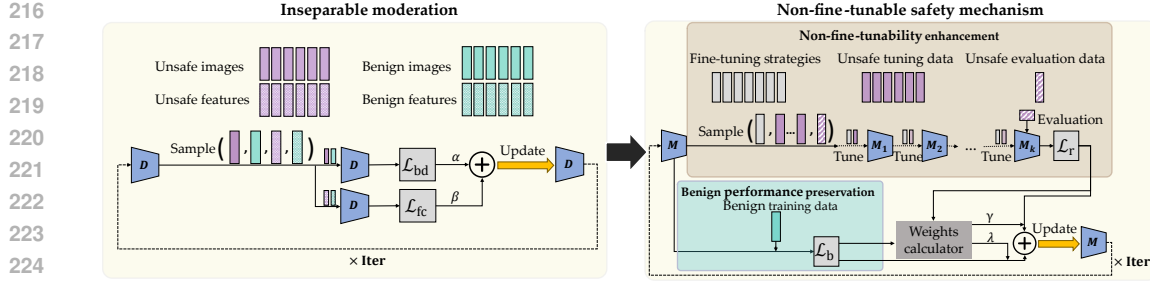


Figure 2: Design of PATRONUS. PATRONUS mainly consists of two processes, *i.e.*, the fine-tuning (FTS) loops and the normal training reinforcement (NTR) loops. The FTS loops are designed to simulate different fine-tuning processes and degrade the fine-tuning performance in the restricted domain. The NTR loops are designed to maintain the performance in the original domain. The number of tasks N , the number of updates K , the learning rates of FTS loops α and NTR loops β , and the number of FTS loops ℓ_{FTS} and NTR loops ℓ_{NTR} , and the total number of iterations Iter are hyper-parameters.

$$\mathcal{M}'_{dec}(f^t) = \begin{cases} \emptyset & \text{if } \mathcal{F}_{emb}(f^t) = \text{False}, \\ \mathcal{M}_{dec}(f^t) & \text{if } \mathcal{F}_{emb}(f^t) = \text{True}. \end{cases}$$

Where $\mathcal{F}_{emb}(f^t) = \text{True}$ (or False) signifies that the moderator regards f^t as a safe (or unsafe) feature. \odot denotes the AND operation. f^t is the feature generated by the diffusion corresponding to textual input x^t , obtained by

$$f^t = (\mathcal{M}_{diff} \circ \mathcal{M}_{enc})(x^t). \quad (10)$$

Developing such a conditional decoder is far from trivial. We achieve it by fine-tuning the pre-trained decoder with the combined loss from two processes, *i.e.*, the conditional decoding process, and the feature calibration process as

$$\mathcal{L}_{\text{im}} = \alpha \cdot \mathcal{L}_{\text{cd}} + \beta \cdot \mathcal{L}_{\text{fsc}}. \quad (11)$$

4.2.1 CONDITIONAL DECODING

We perform an image-oriented alignment to direct the decoder to decode unsafe features into zero vectors while ensuring its decoding behaviors for benign features remain intact, which we describe as conditional decoding. Given the pre-trained VAE, consisting of a encoder \mathcal{E} parameterized by ϕ and a decoder \mathcal{D} parameterized by θ . They were trained with the objective function as

$$\mathcal{L}(\theta, \phi) = -\mathbb{E}_{z \sim q_\phi(z|x)} [\log p_\theta(x|z)] + \text{KL}(q_\phi(z|x) || p(z)). \quad (12)$$

Optimizing the first loss brings \mathcal{D} the conditional generation capability, opening up the possibility for us to achieve conditional decoding. We assume the benign images and unsafe images follow distinctly distinguishable distributions, \mathbb{X}_n and \mathbb{X}_u . Thus, the complete encoder feature space \mathbb{Z} can also be divided into benign space and unsafe space, as

$$\mathbb{Z} = \mathbb{Z}_n \cup \mathbb{Z}_u = q_{\phi, x \sim \mathcal{X}_n}(z|x) \cup q_{\phi, x \sim \mathcal{X}_u}(z|x). \quad (13)$$

Then we fine-tune the decoder with the loss function like

$$\mathcal{L}(\theta, \phi) = -\mathbb{E}_{z \sim \mathbb{Z}_n} [\log p_\theta(x|z)] - \mathbb{E}_{z \sim \mathbb{Z}_u} [\log p_\theta(\mathbf{0}|z)]. \quad (14)$$

The former term guarantees the reconstruction performance for benign features, and the latter term encourages the decoder to decode the unsafe features to zero-vectors. In practice, we describe $\log p_\theta(x|z)$ through the Mean Square Error (MSE). Then the loss of the decoder is crafted as

$$\mathcal{L}(\mathcal{D}_\theta) = \alpha \cdot \frac{1}{|\mathbb{X}_n|} \sum_i \mathcal{L}_{\text{MSE}}(\mathcal{D}_\theta(\mathcal{E}_\phi(x_i)), x_i) + \beta \cdot \frac{1}{|\mathbb{X}_u|} \sum_j \mathcal{L}_{\text{MSE}}(\mathcal{D}_\theta(\mathcal{E}_\phi(x_j)), \mathbf{0}), \quad (15)$$

where $\mathcal{D}_\theta(\mathcal{E}_\phi(\cdot))$ is the encode-decode process. \mathbb{X}_n and \mathbb{X}_u are the defender's training sets of benign and unsafe images. α, β controls the weights to combine these two terms.

However, forcing the decoder to map the unsafe features to zeros is strict and superfluous. In fact, we only need to corrupt the decoding outputs from the semantic level, *e.g.*, fuzzy or mosaicked. To this end, we propose the smoothed biased decoding inspired by the VGG perceptual loss in (Johnson

et al., 2016). Specifically, we modify the second term in Equation 15 and get final **conditional decoding loss** as

$$\mathcal{L}_{\text{cd}}(\mathcal{D}_\theta) = \alpha \cdot \frac{1}{|\mathbb{X}_n|} \sum_i \mathcal{L}_{\text{MSE}}(\mathcal{D}_\theta(\mathcal{E}_\phi(x_i)), x_i) + \beta \cdot \frac{1}{|\mathbb{X}_u|} \sum_j \mathcal{L}_{\text{VGG}}(\mathcal{D}_\theta(\mathcal{E}_\phi(x_j)), \mathbf{0}), \quad (16)$$

where $\mathcal{L}_{\text{VGG}}(x, \mathbf{0})$ is the smoothed denial-of-service loss that is calculated by

$$\mathcal{L}_{\text{VGG}}(x, \mathbf{0}) = \mathcal{L}_{\text{MSE}}(\text{VGG}(x), \text{VGG}(\mathbf{0})), \quad (17)$$

where $\text{VGG}(\cdot)$ is the feature extractor from the pre-trained VGG-19 model (Simonyan & Zisserman, 2014). We empirically verify that constraining unsafe outputs to be close to zero in the VGG’s feature space rather than in the pixel space exhibits less impact on the benign decoding functionality and more stable and generalizable corruption performance of unsafe outputs. Furthermore, since the VGG’s feature space aligns with human-perceived attributes (Johnson et al., 2016), ensuring the unlearning effect for unsafe features achieves our intended purpose.

4.2.2 FEATURE SPACE CALIBRATION

However, there is a gap between the feature distributions of the encoder output and the diffusion output, leading to PATRONUS’s occasional failure in the practical T2I working scenario. We design a feature space calibration to fix the gap, thus generalizing the unlearnability from the encoder feature space to the diffusion feature space. Inspired by the idea of classifier-free guidance (Ho & Salimans, 2022), we introduce text-conditioned features to participate in the conditional decoder’s training process.

Specifically, we utilize a caption model \mathcal{C} , e.g., LLaVa (Liu et al., 2024), to generate a text description for each image x_i in \mathbb{X}_u and \mathbb{X}_n to serve as the pseudo prompts p_i . We input these pseudo prompts into the conditioning module and collect the diffusion outputs to build unsafe and benign diffusion feature set \mathbb{F}_u and \mathbb{F}_n as follows

$$\begin{aligned} \mathbb{P}(\mathcal{X}) &= \{p_1, p_2, \dots, p_n\} = \{\mathcal{C}(x_i | x_i \in \mathbb{X})\}_{i=1,2,\dots,n}, \\ \mathbb{F}(\mathbb{P}, \epsilon_\psi) &= \{f_1, f_2, \dots, f_n\} = \{\epsilon_\psi(c_i, z_i)\}_{i=1,2,\dots,n}, \end{aligned} \quad (18)$$

where ϵ_ψ is the diffusion module’s denoising function parameterized by a U-Net with parameter ψ , c_j is the conditional vector obtained by inputting the j -th pseudo prompt into the text encoder, z_j is the initial noise.

We compute the **feature-calibration loss** by

$$\mathcal{L}_{\text{fc}} = \frac{1}{|\mathbb{F}_u|} \sum_{f_j \in \mathbb{F}_u} \mathcal{L}_{\text{VGG}}(\mathcal{D}_\theta(f_j), \mathbf{0}) + \frac{1}{|\mathbb{F}_n|} \sum_{f_i \in \mathbb{F}_n} \mathcal{L}_{\text{MSE}}(\mathcal{D}_0(f_i), \mathcal{D}_\theta(f_i)), \quad (19)$$

which is combined with the Biased-Decoding loss Equation 16 for fine-tuning the decoder in the image-oriented alignment process. Note that we use the original decoder \mathcal{D}_0 ’s output as the supervision in the second term for two reasons: 1) the original decoder operates well in the diffusion module’s feature space; thus it can instruct the feature calibration, and 2) the original decoder has intact benign knowledge, minimizing this loss encourages \mathcal{D}_θ to continuously review the benign knowledge with the supervision from the teacher \mathcal{D}_0 .

4.3 NON-FINE-TUNABLE SAFETY MECHANISM

As previously discussed, model alignment defenses fail to withstand malicious fine-tuning, and so does our conditional decoder obtained in the last section. To mitigate this vulnerability of alignment models (e.g., the conditional decoder and the aligned U-Net Li et al., 2024; Schramowski et al., 2023; Gandikota et al., 2023), we design an innovative non-fine-tunable safety mechanism, which consists of two parts, i.e., the non-fine-tunability enhancement and the benign performance preservation. The non-fine-tunable safety mechanism combines these two losses and optimizes the model with the objective

$$\mathcal{L}_{\text{nft}} = \gamma \cdot \mathcal{L}_{\text{ftr}} + \lambda \cdot \mathcal{L}_{\text{bpp}}, \quad (20)$$

where γ and λ are dynamic coefficients computed by an adaptive weights calculator introduced in Appendix D.

324 4.3.1 NON-FINE-TUNABILITY ENHANCEMENT
 325

326 In this section, we discuss the proposed non-fine-tunability enhancement and its instantiations for
 327 the decoder and diffusion modules.

328 We investigate our goal through the lens of game theory. Take a model (a decoder or a diffusion mod-
 329 el) \mathcal{M} as instance, the game between the fine-tuning adversary and the defender can be formulated
 330 as a min-max problem like

331
 332
$$\max_{\mathcal{M}} \mathcal{L} \left(\min_{\phi' \in \Phi'} \mathcal{L}_{\text{MSE}} (\phi' (\mathcal{M}, \mathbb{X}_m), \mathbb{X}_m) \right), \quad (21)$$

 333

334 where Φ is the fine-tuning strategy set, \mathbb{X}_m is an unsafe data set. In the inner optimization, the
 335 adversary tries to fine-tune our model to a state that performs well in the unsafe domain. In the outer
 336 optimization, the defender corrupts the states obtained in the inner optimization.

337 Since we do not assume to know \mathbb{X}_m and Φ' , we leverage the concept of adversarial training to
 338 approximate Equation 21. The key to adversarial training is simulating the worst-case adversary
 339 in the inner optimization and countering that adversary in the outer optimization. Following this
 340 guideline, we craft the following min-max problem to fulfill our goal
 341

342
$$\max_{\mathcal{M}} \mathcal{L} \left(\min_{\phi \in \Phi} \mathcal{L}_{\text{MSE}} (\phi (\mathcal{M}, \mathbb{X}_{\text{tune}}), \mathbb{X}_{\text{eval}}) \right), \quad (22)$$

 343

344 where \mathbb{X}_{tune} is the fine-tuning set for inner fine-tuning and \mathbb{X}_{eval} is the evaluation set for outer
 345 evaluation. They both come from the defender's unsafe data set \mathbb{X}_u , which is sampled from the
 346 unsafe domain. Φ is our simulated fine-tuning strategy set.

347 Since the max problem in Equation 22 solving is hard to converge, we instead seek to solve the
 348 following min-min problem
 349

350
$$\min_{\mathcal{M}} \mathcal{L}_D \left(\min_{\phi \in \Phi} \mathcal{L}_{\text{MSE}} (\phi (\mathcal{M}, \mathbb{X}_{\text{tune}}), \mathbb{X}_{\text{eval}}), \mathbf{0} \right), \quad (23)$$

 351

352 where \mathcal{L}_D is a surrogate loss function, which satisfies that minimizing itself shares the similar goal
 353 with maximizing the original MSE loss, *i.e.*, disrupting the unsafe outputs. For instance, we can
 354 minimize the distance between the model's output and zero vectors, like the biased decoding loss 16
 355 in Section §4.2.
 356

357 The inner objective represents that the simulated adversary meticulously crafts the fine-tuning strate-
 358 gies to fine-tune our model with the unsafe data \mathbb{X}_{tune} . The outer objective represents the defender
 359 expects the fine-tuned model to still decode the unsafe images to smoothed zero vectors.

360 To solve this min-min problem, we utilize the pipeline from (Deng et al., 2024). In practice, we
 361 repeat and alternate between inner and outer optimization: At the beginning of each iteration, let
 362 \mathcal{M}_0 denote the decoder's parameters. First, we use \mathbb{X}_{tune} and strategy ϕ to fine-tune \mathcal{M}_0 and get
 363 the resulting state \mathcal{M}_1 as

364
$$\mathcal{M}_1 = \phi (\mathcal{M}_0, \mathbb{X}_{\text{tune}}). \quad (24)$$

365 Then, we use \mathbb{X}_{eval} to evaluate \mathcal{M}_1 's performance and calculate the **fine-tuning-resistance loss** \mathcal{L}_{ftr}
 366 that measures the discrepancy between the current performance and the desired ones, *e.g.*, outputting
 367 zeros when taking the unsafe features as inputs.

368 Finally, we update \mathcal{M}_0 with this loss by doing
 369

370
$$\theta_0 \leftarrow \theta_0 - \eta \cdot \nabla_{\theta_0} \mathcal{L}_{\text{ftr}} (\mathcal{M}_1, \mathbb{X}_{\text{eval}}), \quad (25)$$

371 where θ_0 is the parameters of \mathcal{M}_0 and η is the learning rate of the outer optimization.

372 To save the memory requirements, we turn to first-order approximation (Finn et al., 2017) and update
 373 \mathcal{M}_0 as follows

374
$$\theta_0 \leftarrow \theta_0 - \eta \cdot \nabla_{\theta_0} \mathcal{L}_{\text{ftr}} (\mathcal{M}_1, \mathbb{X}_{\text{eval}}), \quad (26)$$

375 That is, we use the gradients with respect to \mathcal{M}_1 to approximate the gradients with respect to \mathcal{M}_0 .
 376 Note that the true update to the model is implemented in Equation 26, while the updation between
 377 \mathcal{M}_0 and \mathcal{M}_1 is merely for calculating \mathcal{L}_{ftr} and does not modify the model's existent parameters.

378 Equation 26 makes the model learn the ability to perform poorly when fine-tuned with the unsafe
 379 data.

380 **Mixed Sampling Strategy:** To improve PATRONUS’s robustness against different fine-tuning pro-
 381 cesses, we propose a mixed sampling strategy for the inner loop. To be specific, we construct a bag
 382 of fine-tuning strategies containing various optimizers, learning rates, batch sizes, fine-tune sizes,
 383 and iteration numbers. Each time, we sample a fine-tuning strategy for the inner loop.

384 The focus of the bag of fine-tuning strategies is on the selection of the optimizer. To ensure effi-
 385 ciency and effectiveness, we include two optimizers in the inner optimization, *i.e.*, SGD (Robbins
 386 & Monro, 1951) and Adam (Kingma & Ba, 2015). These two optimizers have complementary dy-
 387 namic characteristics, *i.e.*, SGD is better at escaping local optima, while Adam is better at escaping
 388 saddle points (Xie et al., 2022). By resisting these two optimizers in the outer optimization, we are
 389 able to move our defense model to a state that is difficult to escape and performs poorly on unsafe
 390 data.

391 For other super-parameters like learning rates and batch sizes, we include all commonly used ranges.
 392 For fine-tuning size and iteration number, we sample from an excessive range for what is normally
 393 required for fine-tuning. We refer to the Appendix G for detailed instantiations of non-fine-tunable
 394 decoders and diffusion modules.

396 4.3.2 BENIGN PERFORMANCE PRESERVATION

398 There is a conflict between the refusal outputs for unsafe inputs and the intact outputs for benign
 399 inputs. To preserve the benign performance, we calculate the loss \mathcal{L}_{bpp} on benign data and it is then
 400 combined with the fine-tuning-resistance \mathcal{L}_{ftr} loss for joint optimization. For the decoder \mathcal{M}_{dec} , we
 401 compute

$$402 \quad \mathcal{L}_{\text{bpp}} = \frac{1}{|\mathbb{X}_n|} \sum_{x_i \in \mathbb{X}_n} \mathcal{L}_{\text{MSE}}(\mathcal{M}_{\text{dec}}(\mathcal{E}(x_i)), x_i) + \frac{1}{|\mathbb{F}_n|} \sum_{f_i \in \mathbb{F}_n} \mathcal{L}_{\text{MSE}}(\mathcal{M}_{\text{dec}}^0(f_i), \mathcal{M}_{\text{dec}}(f_i)), \quad (27)$$

405 where the $\mathcal{M}_{\text{dec}}^0$ is the original decoder, \mathcal{E} is the corresponding encoder from the VAE. x_i is benign
 406 image and f_i is its corresponding diffusion feature (refer to Section §4.2.2). The two terms in Equa-
 407 tion 27 encourage the decoder to preserve the benign knowledge in encoder and diffusion feature
 408 spaces, respectively.

409 For the diffusion module, we compute

$$411 \quad \mathcal{L}_{\text{bpp}} = \frac{1}{|\mathbb{X}_n|} \sum_{x_i \in \mathbb{X}_n} \mathcal{L}(\epsilon_\theta(\hat{x}_i, c_i, t), z), \quad (28)$$

414 where \hat{x}_i, c_i, t, z are the noisy benign image, conditioning vector from its corresponding caption,
 415 timestep, and the ground-truth noise, respectively. Optimizing Equation 28 essentially replicates
 416 U-Net’s standard training process, which can effectively preserve the benign performance.

418 5 EVALUATION

420 5.1 EXPERIMENT SETUP

422 **Implementation.** We have implemented a prototype of PATRONUS on the PyTorch (Paszke et al.,
 423 2019) platform according to Algorithm 1 using 4 A100-80GB GPUs (NVIDIA). We choose Sta-
 424 ble Diffusion (version 1.4) as the experiment subject following previous work (Yang et al., 2023;
 425 Gandikota et al., 2023; Li et al., 2024). For the sake of brevity, we refer to the Appendix E for
 426 detailed information on PATRONUS’ implementation.

427 **Datasets.** Our experiment involves six datasets, including two image datasets, *i.e.*, ImageNet and
 428 NSFW dataset, used in PATRONUS’s training process, two sexual-explicit prompt datasets, *i.e.*, I2P
 429 and SneakyPrompt, and one sexual-explicit image-caption dataset, *i.e.*, NSFW-prompt, for eval-
 430 uating the defensive performance of the PATRONUS, and a benign prompt dataset from MS COCO
 431 caption dataset for verifying the intactness of benign performance. We refer to the Appendix A for
 detailed information on these datasets.

432 **Metrics.** Our experiments involve two metrics that are widely applied in the T2I scenario, *i.e.*,

- 433
- 434 • **CLIP Score.** The CLIP score assesses the correlation between the image and the corre-
435 sponding text. It is calculated by the average cosine similarity between the given CLIP
436 text embedding and its generated CLIP image embedding. A higher score is desirable for
437 benign prompts; the opposite is true for unsafe prompts.
 - 438 • **MSE Error.** For the malicious fine-tuning adversary, we evaluate the fine-tuned model’s
439 test loss, illustrating the degree to which the model is optimized in the fine-tuning process.
440 Both the decoder and the diffusion module employ MSE Error as their loss function.

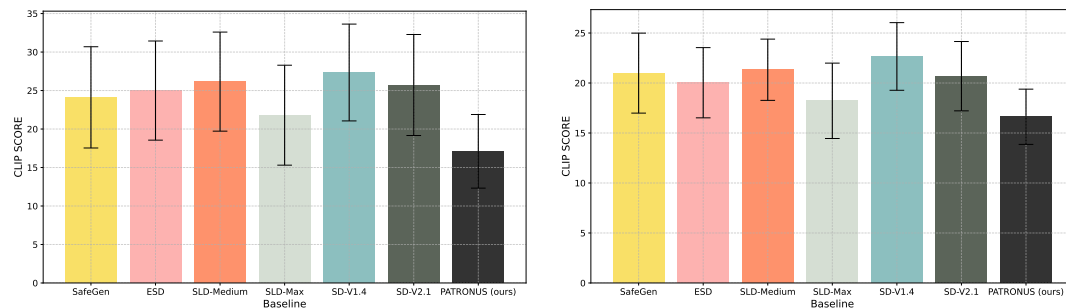
441 **Baselines.** We compare PATRONUS with five baselines, including SD-V1.4, SD-V2.1, and SLD,
442 and two state-of-the-art model alignment methods, including ESD and SafeGen. We refer to the
443 Appendix C for detailed information on these baselines.

445 5.2 OVERALL PERFORMANCE

446 In this section, we evaluate the overall performance of PATRONUS compared with baselines. We
447 consider two types of adversaries: 1) the direct prompting adversary who directly prompts the model
448 with unsafe content without modifying its parameters, and 2) the malicious fine-tuning adversary
449 who performs a malicious fine-tuning then prompting.

451 5.2.1 DEFEND AGAINST DIRECT PROMPTING ADVERSARY

452 This part discusses the defending against the direct prompting adversary. Two representative prompt-
453 ing methods are I2P and SneakyPrompt. Specifically, we employ I2P and SneakyPrompt to query
454 the models and evaluate the CLIP score of the generated images. We present the results in Figure 3
455 and Figure 4. We can see that PATRONUS achieves the lowest CLIP score compared with the base-
456 lines, meaning that PATRONUS generates minimal unsafe content when being maliciously prompted
457 (Figure 3), with even stronger adversarial prompting (Figure 4).



470 Figure 3: Effectiveness of PATRONUS’s defend-
471 ing against I2P attack compared with six base-
472 lines. Attacking PATRONUS yields the lowest
473 CLIP score.

470 Figure 4: Effectiveness of PATRONUS’s defend-
471 ing against SneakyPrompt attack compared with six
472 baselines. Attacking PATRONUS yields the lowest
473 CLIP score.

474 5.2.2 DEFEND AGAINST MALICIOUS FINE-TUNING ADVERSARY

475 Existing work focuses on the threat model like Section §5.2.1, ignoring a realistic but aggressive
476 scenario where the adversary fine-tunes the models with unsafe data before prompting. This section
477 considers the circumstances where the adversary has no knowledge of our defense mechanisms. For
478 instance, in a common scenario, we release our model without sharing defense-related information.
479 Consistent with the usual practice of fine-tuning SD models (*e.g.*, the widely-used diffusers library
480 (von Platen et al., 2022) defaults to fine-tuning the U-Net and does not even provide an interface
481 for fine-tuning other modules), the adversary typically opts to fine-tune the U-Net module. We
482 designate this type of adversary as the naive fine-tuning adversary, and we discuss adaptive fine-
483 tuning adversaries with more prior knowledge in Section H.

484 To assess the performance of PATRONUS and baselines against this type of adversary, we fine-tune
485 their U-Nets on 200 Porn image-caption pairs from NSFW-prompt for 20 iterations. Then, we
use I2P prompt set to query the fine-tuned model and examine the changing trends of the CLIP

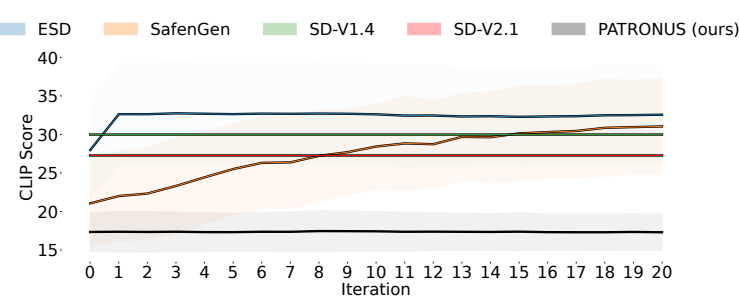


Figure 5: Effectiveness of PATRONUS’s resisting malicious fine-tuning compared with four baselines. PATRONUS ensures that the CLIP score on unsafe generations remains consistently low and does not increase as fine-tuning progresses.

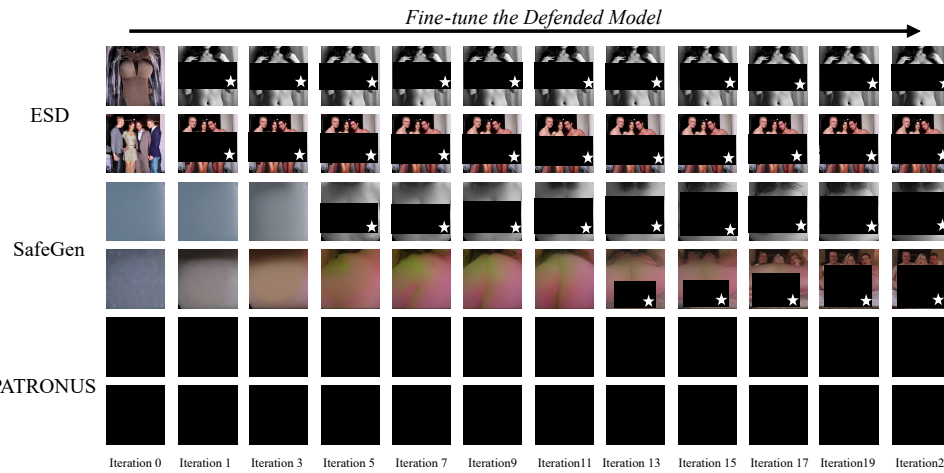


Figure 6: Effectiveness of PATRONUS’s resisting malicious fine-tuning compared with four baselines. PATRONUS ensures that the outputs regarding unsafe prompts remain zeros as fine-tuning progresses.

score and the visual results with respect to the number of fine-tuning iterations. A larger CLIP score means more unsafe content in the generated images. From Figure 5, we can see the CLIP scores of SD-V1.4 and SD-V2.1 are high enough from the very beginning, proving the adversarial prompts’ effectiveness. The CLIP scores of ESD and SafeGen are low initially, suggesting their effectiveness in defending against adversarial prompts. However, after only a few iterations, their CLIP scores rapidly increase, revealing their vulnerability against malicious fine-tuning. We present the corresponding visual results in Figure 6. As we can see, the CLIP scores of PATRONUS remain low during the whole fine-tuning process, and the generated images are always devoid of unsafe content.

5.3 PRESERVING BENIGN PERFORMANCE

In this part, we evaluate the benign performance of benign prompts. Following the existing work, we use captions from MS COCO dataset as benign prompts and examine the CLIP scores. From Figure F, we can see PATRONUS’s CLIP scores are comparable to other baselines, demonstrating PATRONUS does not introduce extra degradation on the benign performance.

6 CONCLUSION

In this paper, we introduce an innovative defense PATRONUS for pre-trained T2I models, which includes an inseparable moderator and a non-fine-tunable safety mechanism. PATRONUS resolves the drawbacks of existing defenses that fail to remain effective in white-box scenarios. Our experiments have validated the efficacy of PATRONUS in refusing unsafe prompting and resisting malicious fine-tuning as well as its intact benign performance.

540 REFERENCES
541542 Midjourney. <https://www.midjourney.com>.543 AIML-TUDA. Inappropriate image prompts (i2p). <https://huggingface.co/datasets/544 AIML-TUDA/i2p>.545 Artificial Intelligence & Machine Learning Lab at TU Darmstadt. Inappropriate image prompts
546 (i2p), n.d. URL <https://huggingface.co/datasets/546 AIML-TUDA/i2p>. Accessed:
547 2024-09-29.548 Evgeniy Bazarov. Nsfw data source urls. https://github.com/EBazarov/nsfw_data_549 source_urls, 2018.550 Jia Deng, Wei Dong, Richard Socher, Li-Jia Li, Kai Li, and Li Fei-Fei. Imagenet: A large-scale
551 hierarchical image database. In *2009 IEEE Computer Society Conference on Computer Vision and*
552 *Pattern Recognition (CVPR 2009), 20-25 June 2009, Miami, Florida, USA*, pp. 248–255. IEEE
553 Computer Society, 2009. doi: 10.1109/CVPR.2009.5206848. URL <https://doi.org/10.1109/CVPR.2009.5206848>.554 Jiangyi Deng, Shengyuan Pang, Yanjiao Chen, Liangming Xia, Yijie Bai, Haiqin Weng, and
555 Wenyuan Xu. Sophon: Non-fine-tunable learning to restrain task transferability for pre-trained
556 models. In *2024 IEEE Symposium on Security and Privacy (SP)*, pp. 250–250. IEEE Computer
557 Society, 2024.558 Jean-Antoine Désidéri. Multiple-gradient descent algorithm (mgda) for multiobjective optimization.
559 *Comptes Rendus Mathematique*, 350(5-6):313–318, 2012.560 Chelsea Finn, Pieter Abbeel, and Sergey Levine. Model-agnostic meta-learning for fast adaptation
561 of deep networks. In *International Conference on Machine Learning*. PMLR, 2017.562 Rohit Gandikota, Joanna Materzynska, Jaden Fiotto-Kaufman, and David Bau. Erasing concepts
563 from diffusion models. In *Proceedings of the IEEE/CVF International Conference on Computer*
564 *Vision*, pp. 2426–2436, 2023.565 Jonathan Ho and Tim Salimans. Classifier-free diffusion guidance. *arXiv preprint*
566 *arXiv:2207.12598*, 2022.567 Edward J Hu, Yelong Shen, Phillip Wallis, Zeyuan Allen-Zhu, Yuanzhi Li, Shean Wang, Lu Wang,
568 and Weizhu Chen. Lora: Low-rank adaptation of large language models. *arXiv preprint*
569 *arXiv:2106.09685*, 2021.570 Tatum Hunter. AI porn is easy to make now. for women, that's a nightmare.
571 [https://www.washingtonpost.com/technology/2023/02/13/
572 ai-porn-deepfakes-women-consent](https://www.washingtonpost.com/technology/2023/02/13/ai-porn-deepfakes-women-consent), 2023a.573 William Hunter. Paedophiles are using AI to create sexual images of celebrities as children, report finds.
574 <https://www.dailymail.co.uk/sciencetech/article-12669791/Paedophiles-using-AI-create-sexual-images-celebrities-CHILDREN-report-finds.html>,
575 2023b.576 OpenAI Inc. Dall-e 2. <https://openai.com/dall-e-2>.577 Michelle Jieli. Nsfw text classifier. [https://huggingface.co/michellejieli/NSFW_578 text_classifier?not-for-all-audiences=true](https://huggingface.co/michellejieli/NSFW_text_classifier?not-for-all-audiences=true).579 Justin Johnson, Alexandre Alahi, and Li Fei-Fei. Perceptual losses for real-time style transfer and
580 super-resolution. In *Computer Vision–ECCV 2016: 14th European Conference, Amsterdam, The*
581 *Netherlands, October 11–14, 2016, Proceedings, Part II* 14, pp. 694–711. Springer, 2016.582 Diederik P. Kingma and Jimmy Ba. Adam: A method for stochastic optimization. In *International*
583 *Conference on Learning Representations*. OpenReview.net, 2015.

- 594 Junnan Li, Dongxu Li, Silvio Savarese, and Steven Hoi. Blip-2: Bootstrapping language-image
 595 pre-training with frozen image encoders and large language models. In *International conference*
 596 *on machine learning*, pp. 19730–19742. PMLR, 2023.
- 597
 598 Michelle Li. Nsfw text classifier on hugging face. [https://huggingface.co/
 599 michellejieli/NSFW-text-classifier](https://huggingface.co/michellejieli/NSFW-text-classifier).
- 600 Xinfeng Li, Yuchen Yang, Jiangyi Deng, Chen Yan, Yanjiao Chen, Xiaoyu Ji, and Wenyuan Xu.
 601 Safegen: Mitigating sexually explicit content generation in text-to-image models. In *Proceedings*
 602 *of the 2024 ACM SIGSAC Conference on Computer and Communications Security (CCS)*, 2024.
- 603 Tsung-Yi Lin, Michael Maire, Serge Belongie, James Hays, Pietro Perona, Deva Ramanan, Piotr
 604 Dollár, and C Lawrence Zitnick. Microsoft coco: Common objects in context. In *Computer*
 605 *Vision–ECCV 2014: 13th European Conference, Zurich, Switzerland, September 6–12, 2014,*
 606 *Proceedings, Part V 13*, pp. 740–755. Springer, 2014.
- 607
 608 Haotian Liu, Chunyuan Li, Yuheng Li, and Yong Jae Lee. Improved baselines with visual instruction
 609 tuning. In *Proceedings of the IEEE/CVF Conference on Computer Vision and Pattern Recog-
 610 nition*, pp. 26296–26306, 2024.
- 611 M. V. L. G. LMU. Safety checker. [https://huggingface.co/CompVis/
 612 stable-diffusion-safety-checker](https://huggingface.co/CompVis/stable-diffusion-safety-checker), a.
- 613
 614 M. V. L. G. LMU. Stable diffusion v1-4. [https://huggingface.co/CompVis/
 615 stable-diffusion-v1-4](https://huggingface.co/CompVis/stable-diffusion-v1-4), b.
- 616 Madison McQueen. AI porn is here and it's dangerous. [https://exoduscry.com/
 617 articles/ai-porn](https://exoduscry.com/articles/ai-porn), 2023.
- 618 Dan Milmo. AI-created child sexual abuse images ‘threaten to overwhelm inter-
 619 net’. [https://www.theguardian.com/technology/2023/oct/25/
 620 ai-created-child-sexual-abuse-images-threaten-overwhelm-internet](https://www.theguardian.com/technology/2023/oct/25/ai-created-child-sexual-abuse-images-threaten-overwhelm-internet), 2023.
- 621
 622 new-workspace bjaa4. 3clase dataset. [https://universe.roboflow.com/
 623 new-workspace-bjaa4/3clase](https://universe.roboflow.com/new-workspace-bjaa4/3clase), jul 2022. URL [https://universe.roboflow.com/
 624 new-workspace-bjaa4/3clase](https://universe.roboflow.com/new-workspace-bjaa4/3clase). visited on 2024-07-02.
- 625
 626 Adam Paszke, Sam Gross, Francisco Massa, Adam Lerer, James Bradbury, Gregory Chanan, Trevor
 627 Killeen, Zeming Lin, Natalia Gimelshein, Luca Antiga, Alban Desmaison, Andreas Köpf, Ed-
 628 ward Z. Yang, Zachary DeVito, Martin Raison, Alykhan Tejani, Sasank Chilamkurthy, Benoit
 629 Steiner, Lu Fang, Junjie Bai, and Soumith Chintala. PyTorch: An imperative style, high-
 630 performance deep learning library. In *Conference on Neural Information Processing Systems*.
 631 PMLR, 2019.
- 632
 633 Alec Radford, Jong Wook Kim, Chris Hallacy, Aditya Ramesh, Gabriel Goh, Sandhini Agarwal,
 634 Girish Sastry, Amanda Askell, Pamela Mishkin, Jack Clark, et al. Learning transferable visual
 635 models from natural language supervision. In *International conference on machine learning*, pp.
 8748–8763. PMLR, 2021.
- 636
 637 Reddit. Tutorial: How to remove the safety filter in 5 seconds. Website, 2022.
 638 URL [https://www.reddit.com/r/StableDiffusion/comments/wv2nw0/
 639 tutorial-how-to-remove-the-safety-filter-in-5/](https://www.reddit.com/r/StableDiffusion/comments/wv2nw0/tutorial-how-to-remove-the-safety-filter-in-5/).
- 640 Herbert Robbins and Sutton Monro. A stochastic approximation method. *The Annals of Mathe-
 641 matical Statistics*, 22(3):400–407, 1951.
- 642
 643 Robin Rombach, Andreas Blattmann, Dominik Lorenz, Patrick Esser, and Björn Ommer. High-
 644 resolution image synthesis with latent diffusion models. In *Proceedings of the IEEE/CVF confer-
 645 ence on computer vision and pattern recognition*, pp. 10684–10695, 2022.
- 646
 647 Patrick Schramowski, Manuel Brack, Björn Deiseroth, and Kristian Kersting. Safe latent diffusion:
 648 Mitigating inappropriate degeneration in diffusion models. In *Proceedings of the IEEE/CVF
 649 Conference on Computer Vision and Pattern Recognition*, pp. 22522–22531, 2023.

648 Karen Simonyan and Andrew Zisserman. Very deep convolutional networks for large-scale image
649 recognition. *arXiv preprint arXiv:1409.1556*, 2014.
650
651 Patrick von Platen, Suraj Patil, Anton Lozhkov, Pedro Cuenca, Nathan Lambert, Kashif Ra-
652 sul, Mishig Davaadorj, Dhruv Nair, Sayak Paul, William Berman, Yiyi Xu, Steven Liu, and
653 Thomas Wolf. Diffusers: State-of-the-art diffusion models. [https://github.com/
654 huggingface/diffusers](https://github.com/huggingface/diffusers), 2022.

655 Rhiannon Williams. Text-to-image AI models can be tricked into generating disturb-
656 ing images. [https://www.technologyreview.com/2023/11/17/1083593/
657 text-to-image-ai-models-can-be-tricked-into-generating-disturbing-images](https://www.technologyreview.com/2023/11/17/1083593/text-to-image-ai-models-can-be-tricked-into-generating-disturbing-images),
658 2023.

659 Zeke Xie, Xinrui Wang, Huishuai Zhang, Issei Sato, and Masashi Sugiyama. Adaptive inertia:
660 Disentangling the effects of adaptive learning rate and momentum. In *International conference
661 on machine learning*, pp. 24430–24459. PMLR, 2022.

663 Yuchen Yang, Bo Hui, Haolin Yuan, Neil Gong, and Yinzhi Cao. Sneakyprompt: Jailbreaking
664 text-to-image generative models. *arXiv preprint arXiv:2305.12082*, 2023.

665
666
667
668
669
670
671
672
673
674
675
676
677
678
679
680
681
682
683
684
685
686
687
688
689
690
691
692
693
694
695
696
697
698
699
700
701

702 **A DATASETS**

703

- 704 • **ImageNet.** ImageNet-1k (Deng et al., 2009) is the most commonly used subset of ImageNet, comprising 1000 object classes and 1,281,167 training images, 50,000 validation images, and 100,000 test images. We denote ImageNet as the benign data for the decoder.
- 705
- 706
- 707 • **MS COCO caption dataset.** MS COCO caption dataset (Lin et al., 2014) contains over 330,000 image-caption pairs regarding common objects. We use it to serve as the benign data, participating in the malicious-fine-tuning resistance process of the diffusion. In line with prior works (Li et al., 2024; Schramowski et al., 2023), we build a benign prompt dataset for evaluating the original performance’s degradation. We prompt GPT in a template like “You are employing a text-to-image model to generate an image. Describe a scene featuring [object], including details of the background, actions, and expressive adjectives.” The [object] is sampled from the categories of ImageNet-1k and MS COCO-2017.
- 708
- 709
- 710 • **NSFW-porn.** NSFW dataset contains five categories, including *porn*, *hentai*, *sexy*, *normal*. Following the existing work, we focus on the porn class, which has about 50,000 images containing porn semantics. We use NSFW-porn images as the unsafe images for processing the decoder.
- 711
- 712
- 713 • **NSFW-prompt.** SafeGen (Li et al., 2024) creates best prompts for 56k real-world instances of sexual exposure (Bazarov, 2018), based on multiple candidate text captioned by BLIP2 (Li et al., 2023). We adopt a subset of this sexually explicit prompt dataset for the adversary’s fine-tuning dataset.
- 714
- 715 • **I2P.** Inappropriate Image Prompts (AIML-TUDA) are comprised of NSFW text prompts manually tailored on lexica.art. that are deliberately crafted to trick the model into outputting unsafe content. We select all sex-related prompts from this source, resulting in a total of 931 samples. We use this dataset to evaluate the defensive performance.
- 716
- 717 • **SneakyPrompt.** SneakyPrompt (Yang et al., 2023) utilizes reinforcement learning to generate prompts that can effectively bypass the moderator and manipulate the model’s output. As a stronger adversarial attack, this dataset is adopted to evaluate the defensive performance.
- 718
- 719
- 720
- 721
- 722
- 723
- 724
- 725
- 726
- 727
- 728
- 729
- 730
- 731

Table 1: Effectiveness of PATRONUS against different optimizers.

Optimizer	Loss in the Unsafe Domain					
	Iteration 0	Iteration 10	Iteration 20	Iteration 30	Iteration 40	Iteration 50
Adade	0.1267 ± 1.0e-4	0.1182 ± 5.5e-4	0.1089 ± 5.9e-4	0.1010 ± 9.7e-4	0.0939 ± 1.2e-3	0.0875 ± 9.5e-4
Adam	0.4093 ± 6.2e-3	0.0978 ± 5.72e-3	0.0577 ± 4.2e-4	0.0503 ± 2.2e-3	0.0324 ± 4.3e-3	0.0189 ± 3.7e-3
Nes	0.2388 ± 6.2e-2	0.3403 ± 7.3e-3	0.3036 ± 1.6e-2	0.2315 ± 8.1e-2	0.1847 ± 7.5e-2	0.1332 ± 6.9e-2
RMS	0.7481 ± 2.2e-1	0.0526 ± 7.0e-3	0.0374 ± 1.6e-2	0.0250 ± 5.1e-3	0.0195 ± 3.0e-3	0.0216 ± 1.2e-2
SGD	0.1807 ± 4.9e-2	0.3427 ± 8.6e-3	0.3075 ± 2.3e-2	0.2541 ± 5.3e-2	0.2033 ± 7.7e-2	0.1549 ± 6.8e-2

Table 2: Effectiveness of PATRONUS against different (potentially) unsafe topics.

Domain	Loss in the Unsafe Domain					
	Iteration 0	Iteration 10	Iteration 20	Iteration 30	Iteration 40	Iteration 50
NSFW-porn	0.1807 ± 4.9e-2	0.3427 ± 8.6e-3	0.3075 ± 2.3e-2	0.02541 ± 5.3e-2	0.2033 ± 7.7e-2	0.1549 ± 6.8e-2
NSFW-sexy	0.0608 ± 3.4e-5	0.0518 ± 3.0e-4	0.0435 ± 8.9e-5	0.0410 ± 2.0e-5	0.0398 ± 7.8e-5	0.0385 ± 2.8e-5
Weapon	0.0333 ± 1.9e-6	0.0322 ± 2.8e-5	0.0308 ± 2.8e-5	0.0298 ± 1.9e-5	0.0291 ± 1.9e-5	0.0285 ± 8.4e-6

Table 3: Effectiveness of PATRONUS against different batch size.

Batch Size	Loss in the Unsafe Domain					
	Iteration 0	Iteration 10	Iteration 20	Iteration 30	Iteration 40	Iteration 50
5	0.2021 ± 5.9e-2	0.3409 ± 1.0e-2	0.3047 ± 2.0e-2	0.2027 ± 9.7e-2	0.1662 ± 8.4e-2	0.1250 ± 8.1e-2
10	0.2418 ± 5.7e-2	0.3216 ± 4.3e-2	0.3101 ± 5.3e-3	0.2606 ± 1.4e-2	0.1813 ± 6.8e-2	0.1180 ± 5.8e-2
15	0.2021 ± 5.9e-2	0.3409 ± 1.0e-2	0.3047 ± 2.0e-2	0.2027 ± 9.7e-2	0.1662 ± 8.4e-2	0.1250 ± 8.1e-2
20	0.1807 ± 4.9e-2	0.3427 ± 8.6e-3	0.3075 ± 2.3e-2	0.2541 ± 5.3e-2	0.2033 ± 7.7e-2	0.1549 ± 6.8e-2
30	0.1854 ± 5.6e-2	0.3400 ± 7.4e-3	0.3055 ± 1.9e-2	0.2257 ± 7.0e-2	0.1923 ± 6.1e-2	0.1038 ± 1.2e-2

756
757
758
759
760
761
762
763
764
765
766
767

Table 4: Effectiveness of PATRONUS against different Finetune number.

Finetune number	Iteration 0	Iteration 10	Iteration 20	Iteration 30	Iteration 40	Iteration 50
100	0.1873 ± 4.1e-2	0.3361 ± 6.3e-3	0.2936 ± 1.4e-2	0.1934 ± 7.9e-2	0.1136 ± 6.2e-2	0.0727 ± 2.5e-2
200	0.1599 ± 3.5e-2	0.3299 ± 3.4e-3	0.2751 ± 3.7e-2	0.1424 ± 8.0e-2	0.0999 ± 7.8e-2	0.0836 ± 6.7e-2
500	0.1807 ± 4.9e-2	0.3427 ± 8.6e-3	0.3075 ± 2.3e-2	0.2541 ± 5.3e-2	0.2033 ± 7.7e-2	0.1549 ± 6.8e-2
1000	0.2263 ± 2.5e-2	0.3009 ± 8.1e-2	0.2619 ± 1.0e-1	0.2001 ± 1.0e-1	0.1443 ± 8.3e-2	0.0959 ± 7.0e-2
2000	0.1806 ± 5.3e-2	0.2742 ± 9.8e-2	0.2056 ± 1.3e-1	0.1425 ± 1.2e-1	0.1211 ± 9.8e-2	0.0942 ± 7.7e-2

772
773
774
775
776
777
778
779
780
781
782
783
784
785
786
787
788
789
790
791
792
793
794

Table 5: Effectiveness of PATRONUS against different learning rate.

Learning Rate	Iteration 0	Iteration 10	Iteration 20	Iteration 30	Iteration 40	Iteration 50
0.001	0.3379 ± 2.3e-2	0.2074 ± 3.0e-2	0.0660 ± 9.7e-3	0.0557 ± 5.8e-3	0.0500 ± 2.4e-3	0.0459 ± 3.0e-3
0.00005	0.1418 ± 2.0e-2	0.1835 ± 8.1e-2	0.1427 ± 9.4e-2	0.0611 ± 2.7e-2	0.0463 ± 5.9e-3	0.0422 ± 3.1e-3
0.0001	0.1807 ± 4.9e-2	0.3427 ± 8.6e-3	0.3075 ± 2.3e-2	0.2541 ± 5.3e-2	0.2033 ± 7.7e-2	0.1549 ± 6.8e-2
0.002	0.3517 ± 1.2e-2	0.1202 ± 3.3e-2	0.0681 ± 1.4e-2	0.0499 ± 1.5e-3	0.0449 ± 3.0e-3	0.0394 ± 2.7e-3
0.00001	0.1272 ± 2.4e-4	0.1174 ± 2.2e-3	0.0974 ± 2.9e-3	0.0818 ± 3.3e-3	0.0695 ± 8.9e-4	0.0616 ± 3.9e-4

800
801
802
803
804
805
806
807
808
809

810 **B ALGORITHM**
811812 **Algorithm 1: PATRONUS**
813

814 **Input:** The benign data \mathcal{X}_n (corresponding benign features \mathcal{F}_n), the unsafe data \mathcal{X}_u (corresponding
815 unsafe features \mathcal{F}_u), the simulated fine-tuning strategies Φ , the encoder \mathcal{E} , MSE loss ℓ .
816 **Input:** The pre-trained decoder \mathcal{D}_0 and U-Net \mathcal{U}_0 , the learning rate α_1 and iterations N_1 for fine-tuning
817 conditional decoder, the learning rate α_2 and iterations N_2 for NFT enhancement of the decoder
818 and U-Net.
819 **Output:** The defended decoder \mathcal{D} , U-Net \mathcal{U}

820 1 . **Initialize** $\mathcal{D}, \mathcal{U} \leftarrow \mathcal{D}_0, \mathcal{U}_0$.
821 2 # Inseparable moderator
822 3 **for** 1 to N_1 **do**
823 4 | **Sample** a batch of $x_u \sim \mathcal{X}_u$, a batch of $f_u \sim \mathcal{F}_u$, a batch of $x_n \sim \mathcal{X}_n$, a batch of $f_n \sim \mathcal{F}_n$.
824 5 | **Compute**
825 6 | $\mathcal{L}_{cd} \leftarrow \ell(\text{VGG}(\mathcal{D}(\mathcal{E}(x_u))), \text{VGG}(0)) + \ell(\mathcal{D}(\mathcal{E}(x_n)), x_n)$ # biased decoding 4.2.1
826 7 | $\mathcal{L}_{fc} \leftarrow \ell(\text{VGG}(\mathcal{D}(f_u)), \text{VGG}(0)) + \ell(\mathcal{D}(f_n), \mathcal{D}_0(f_n))$ # feature space calibration 4.2.2
827 8 | $\mathcal{L}_{im} \leftarrow \alpha \cdot \mathcal{L}_{cd} + \beta \cdot \mathcal{L}_{fc}$
828 9 | **Update** $\mathcal{D} \leftarrow \text{Adam}(\mathcal{D}, \nabla \mathcal{L}_{im}, \alpha_1)$
829 10 **end**
830 11 # Non-fine-tunable safety mechanism
831 12 **for** \mathcal{M} in $[\mathcal{D}, \mathcal{U}]$ **do**
832 13 | **for** 1 to N_2 **do**
833 14 | | **Sample** one fine-tuning setting $\phi \sim \Phi$
834 15 | | **Sample** a batch of $x_{eval} \sim \mathcal{X}_u$, a batch $x_n \sim \mathcal{X}_n$.
835 16 | | **for** $k \leftarrow 1$ to K **do**
836 17 | | | # pseudo fine-tuning
837 18 | | | **Sample** 1 batch of $x_{tune} \sim \mathcal{X}_u$
838 19 | | | **Fine-tune** $\mathcal{M}_{\vartheta}^k \leftarrow \phi(\mathcal{M}_{\vartheta}^{k-1}, x_{tune})$
839 20 | | | **Compute**
840 21 | | | $\mathcal{L}_{i,k} \leftarrow \mathcal{L}_r(\mathcal{M}_{\vartheta}^k, x_{eval})$
841 22 | | **end**
842 23 | | **Compute**
843 24 | | $\mathcal{L}_{ftr} \leftarrow \sum_{k=1}^K \mathcal{L}_{i,k}$ # Non-fine-tunability enhancement 4.3.1
844 25 | | $\mathcal{L}_{bpp} \leftarrow \mathcal{L}_{bpp}(\mathcal{M}, x_n)$ # Benign performance preservation 4.3.2, Note that \mathcal{M} is the statement
845 26 | | before entering the pseudo fine-tuning.
846 27 | | $\gamma, \lambda \leftarrow \text{MGDA}(\mathcal{L}_{ftr}, \mathcal{L}_{bpp})$ # Adaptive weighting D
847 28 | | $\mathcal{L}_{nft} \leftarrow \gamma \cdot \mathcal{L}_{ftr} + \lambda \cdot \mathcal{L}_{bpp}$
848 29 | | **Update** $\mathcal{M} \leftarrow \text{Adam}(\mathcal{M}, \nabla \mathcal{L}_{nft}, \alpha_2)$
849 30 **end**

848 **C BASELINES**
849

- 850 • **SD-V1.4** (LMU, b). In accordance with prior research (Li et al., 2024; Gandikota et al.,
851 2023), we utilize the officially supplied Stable Diffusion V1.4.
- 852 • **SD-V2.1** (at TU Darmstadt, n.d.). Stable Diffusion 2.1 (SD-V2.1) is retrained on cleansed
853 data, where NSFW information is censored by external safety filters.
- 854 • **SLD** (Schramowski et al., 2023). SLD prohibits negative concepts and improves the
855 classifier-free guidance with another diffusion item to shift away from the unsafe domain.
856 We adopt the officially pre-trained model; our configuration examines its four two levels,
857 *i.e.*, medium and max.
- 858 • **ESD** (Gandikota et al., 2023). ESD rectifies sexual concepts such as “nudity” to “[blank]”
859 by fine-tuning the cross-attention layers of U-Net. We reproduce ESD train the model for
860 1000 epochs with a learning rate of 1×10^{-5} , as the paper suggests.
- 861 • **SafeGen** (Li et al., 2024). SafeGen adjusts the diffusion model to corrupt its visual rep-
862 resentations related to pornography. We utilize the released model by SafeGen, which has
863 been evaluated in their paper.

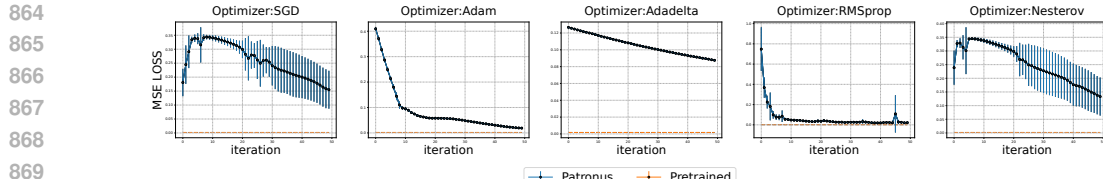


Figure 7: PATRONUS’s effectiveness of decoder protection against different optimizers.

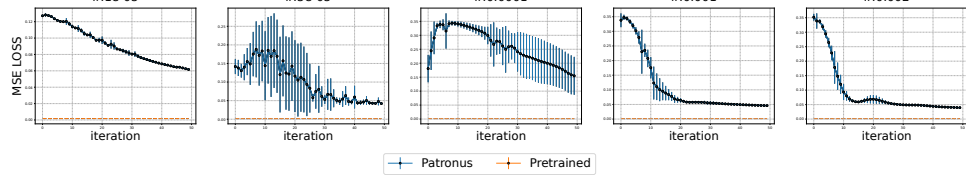


Figure 8: PATRONUS’s effectiveness of decoder protection against different learning rates.

D ADAPTIVE WEIGHTING

In practice, we find it difficult to assign appropriate γ, λ . Therefore, we refer to the Multiple Gradient Descent Algorithm (MGDA), a Multi-task learning technique to optimize a set of (possibly conflicting) objectives (Désidéri, 2012). For tasks $i = 1..k$ with respective losses \mathcal{L}_i , it calculates the gradient (separated from the gradients used by the optimizer) for each single task $\nabla \mathcal{L}_i$ and finds the weighting coefficients $\alpha_1..\alpha_k$ that minimize the sum

$$\min_{\alpha_1, \dots, \alpha_k} \left\{ \left\| \sum_{i=1}^k \alpha_i \nabla \mathcal{L}_i \right\|_2^2 \mid \sum_{i=1}^k \alpha_i = 1, \alpha_i \geq 0 \forall i \right\}. \quad (29)$$

In each iteration of non-fine-tunability enhancement, we obtain \mathcal{L}_{ftr} and \mathcal{L}_{bpp} , then we calculate γ and λ to strike a balance between \mathcal{L}_{ftr} and \mathcal{L}_{bpp} , ensuring that the two tasks *i.e.*, the non-fine-tunable enhancement and the benign performance preservation are simultaneously optimized (or at least not degraded).

E IMPLEMENTATION DETAILS

Given the pre-trained SD model, PATRONUS enhances its decoder and diffusion module and freezes the text encoder. We select the NSFW dataset, especially targeting the porn category, as the unsafe data \mathbb{X}_u . We select ImageNet as the benign data \mathbb{X}_n for the decoder, and COCO as the benign data for the diffusion. We adopt LlaVa-13B (Liu et al., 2024) as the caption model to create pseudo prompts. We set the default PATRONUS configuration as $N_1 = 1200$, $N_2 = 1500$, $\alpha_1 = 5e-5$, $\alpha_2 = 1e-5$, and $K = 20$. The bag of fine-tuning strategies built for the inner optimization contains the sample options: {Momentum, Adam} for the optimizer, $\{5 \times 10^{-5}, 10^{-4}, 10^{-3}, 10^{-2}\}$ for the learning rate, $\{4, 8, 12, 16, 20, 24, 30\}$ for the batch size. These options are determined by balancing efficiency and the effectiveness of simulating the adversary.

F DETAILED PERFORMANCE

G INSTANTIATIONS OF NON-FINE-TUNABILITY ENHANCEMENT

Instantiate Non-fine-tunable Decoder: For the non-fine-tunability enhancement of the decoder \mathcal{M}_{dec} , we designate the conditional decoder obtained in Section §4.2 as the starting point. \mathbb{X}_{tune} and \mathbb{X}_{eval} are unsafe image sets. The fine-tuning-resistance loss is calculated by

$$\mathcal{L}_{\text{ftr}} = \sum_{x_i \in \mathbb{X}_{\text{eval}}} \mathcal{L}_{\text{VGG}}(\mathcal{M}_{\text{dec}}(x_i), \mathbf{0}) + \sum_{f_i \in \mathbb{F}_{\text{eval}}} \mathcal{L}_{\text{VGG}}(\mathcal{M}_{\text{dec}}(f_i), \mathbf{0}), \quad (30)$$

\mathbb{F}_{eval} is \mathbb{X}_{eval} ’s corresponding feature set obtained using the same method described in Section §4.2.2 and used for feature calibration. Optimized with this loss, the decoder learns to decode the unsafe features to smoothed zero vectors after being maliciously fine-tuned.

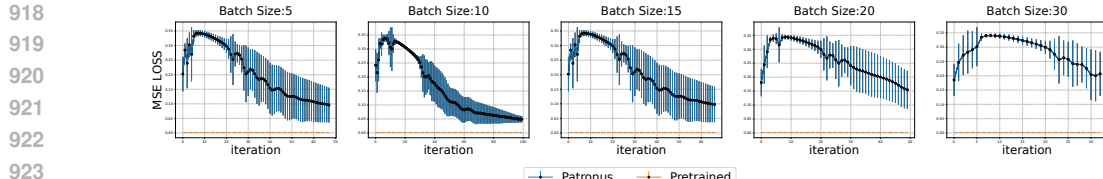


Figure 9: PATRONUS’s effectiveness of decoder protection against different batch sizes.

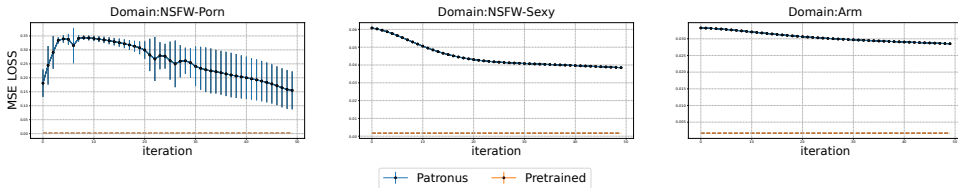


Figure 10: PATRONUS’s effectiveness of decoder protection against different unsafe categories.

Instantiate Non-fine-tunable Diffusion: For the non-fine-tunability enhancement of the diffusion, we designate our aligned U-Net, which is fine-tuned to consistently predict the noise in unsafe images as zero, as the starting point. \mathbb{X}_{tune} and \mathbb{X}_{eval} are unsafe image-caption sets. Consider the U-Net, parameterized by θ (noted as ϵ_θ). ϵ_θ predicts the noises added into the images. The fine-tuning-resistance loss is calculated by

$$\mathcal{L}_{\text{ftr}} = \sum_{x_i \in \mathbb{X}_{eval}} \mathcal{L}(\epsilon_\theta(\hat{x}_i, c_i, t), \mathbf{0}) \quad (31)$$

where c_i is x_i ’s corresponding conditioning vector output by the text encoder. Notably, the starting point we chose here is our own aligned model, though theoretically, our non-fine-tunability enhancement method can be compatible with all alignment techniques, such as Li et al. (2024); Schramowski et al. (2023); Gandikota et al. (2023).

H DEFENDING AGAINST ADAPTIVE ADVERSARY

H.0.1 MALICIOUS FINE-TUNING TOWARDS CONDITIONAL DECODER

In this part, we assume an adaptive adversary who knows that PATRONUS creates a conditional decoder and utilizes the NSFW-*porn* images to implement more aggressive fine-tuning processes on the decoder. To assess PATRONUS’s performance in the worst case, we assume the adversary has already succeeded in compromising the U-Net, leaving only the decoder module to be attacked, *i.e.*, We denote the T2I model with the original U-Net and the conditional decoder as the subject under attack.

We evaluate the robustness of PATRONUS against different fine-tuning strategies, including different optimizers, learning rates, batch sizes, and number of fine-tuning images. We present the MSE losses during the fine-tuning in Figure 7,8,10,11. We can see that PATRONUS introduces significant obstacles to the fine-tuning, making it difficult to converge (resulting in high MSE loss). Simultaneously, it prevents the decoder from generating unsafe content (resulting in always low CLIP scores and corrupted outputs just like Figure 6 shows). Note that PATRONUS shows the robustness against different and unseen fine-tuning settings.

H.0.2 MALICIOUS FINE-TUNING TOWARDS ALIGNED DIFFUSION

In this part, we assume an adaptive adversary who knows that PATRONUS creates a non-fine-tunable aligned diffusion module and utilizes the NSFW-*prompt* image-caption dataset to implement more aggressive fine-tuning processes on the U-Net. To assess PATRONUS’s performance in the worst case, we assume the adversary has already succeeded in compromising the conditional decoder,

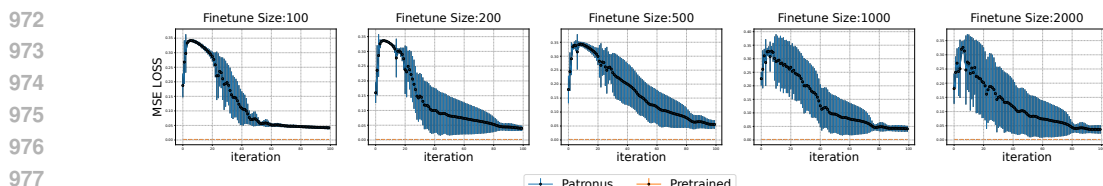


Figure 11: PATRONUS’s effectiveness of decoder protection against different fine-tune sizes.

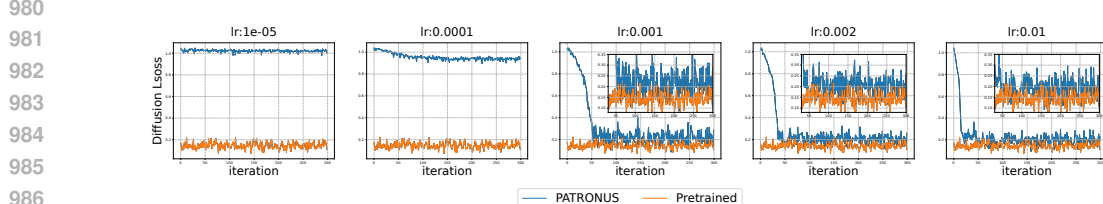


Figure 12: PATRONUS’s effectiveness of U-Net protection against different learning rates.

990
991
992
leaving only the U-Net module to be attacked, *i.e.*, We denote the T2I model with the original
decoder and the defended U-Net as the subject under attack.

993
994
995
996
997
998
999
We assume the adversary utilizes 3000 unsafe image-caption pairs to implement the aggressive
1000 fine-tuning processes on the U-Net. We evaluate the robustness of PATRONUS against different fine-
1001 tuning strategies, including optimizers and learning rates, as shown in 12 and 13. For the learning
1002 rates like $1e - 5, 1e - 4$, PATRONUS leads to the loss remaining nearly unchanged. The bigger
1003 learning rates like $0.001, 0.002, 0.01$ allow the loss to drop quickly, they converge at a larger value,
1004 leaving the model unable to generate unsafe content. We find it is also the case for RMSprop and
1005 Adam optimizers. As for other optimizers, SGD, Adadelta, Nesterov fail to decrease the training
1006 loss. We also assess PATRONUS’s effectiveness in defending LoRA (Low-Rank Adaptation (Hu
1007 et al., 2021)), a popular fine-tuning strategy in the T2I field that introduces two new low-rank param-
1008 eter matrices for fine-tuning. We test different rank values to validate the robustness of PATRONUS,
1009 as shown in Figure 14.

1004 I APPLICABILITY FOR VARIOUS UNSAFE CATEGORIES

1005
1006
Given that existing works are often confined to the pornography category, we take a step further and
1007 evaluate the application potential of PATRONUS against different unsafe categories. We experiment
1008 on NSFW-sexy and the weapon dataset (new-workspace bjaa4, 2022) as the image datasets to im-
1009 plement PATRONUS and follow the similar method of I2P to build unsafe prompt sets for evaluating.
1010 Here, we consider an adaptive adversary as illustrated in Section §H. We present the adversary’s
1011 fine-tuning results in Figure 9. As we can see, PATRONUS also showcases the desired rejection of
1012 unsafe content and resistance to malicious fine-tuning.

1013
1014
1015
1016
1017
1018
1019
1020
1021
1022
1023
1024
1025

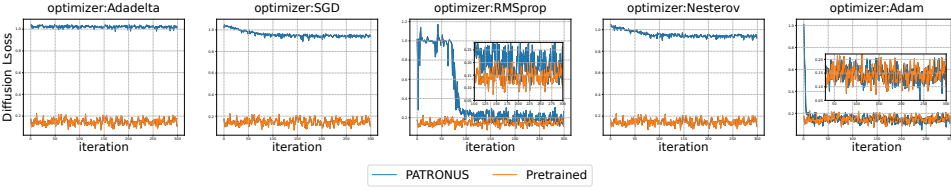


Figure 13: PATRONUS’s effectiveness of U-Net protection against different optimizers.

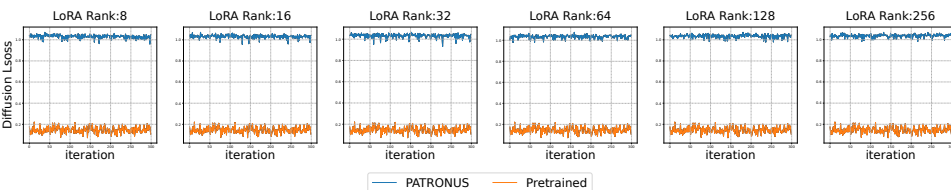


Figure 14: PATRONUS’s effectiveness of U-Net protection against different LoRA ranks

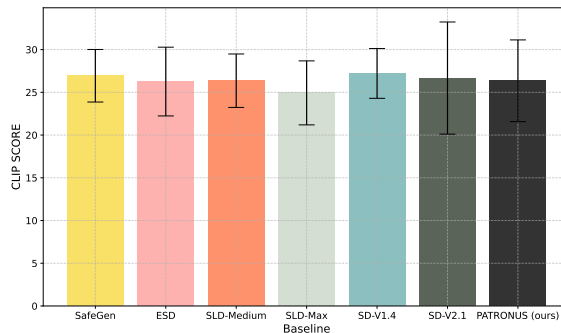


Figure 15: PATRONUS’s intact benign performance.